

Article

# Effectiveness of Multidimensional Controllers Designated to Steering of the Motions of Ship at Low Speed

Witold Gierusz  and Monika Rybczak \* 

Department of Ship Automation, Gdynia Maritime University, 81-225 Gdynia, Poland;  
w.gierusz@we.umg.edu.pl

\* Correspondence: m.rybczak@we.umg.edu.pl; Tel.: +48-506171692

Received: 5 May 2020; Accepted: 15 June 2020; Published: 22 June 2020



**Abstract:** The article described two full multidimensional controllers applied to steer a real vessel named ‘Blue Lady’ that is used by the Foundation for Safety of Navigation and Environment Protection at its training and research facility located at Silm lake in Poland. Both controllers were based on different approaches, but finally gave similar results. The first part describes the object to be controlled which is a training ship used for training of navigators in various conditions, areas and manoeuvres. This is followed by a short description of the theory for both controllers, Robust and Linear Matrix Inequalities (LMI). Next real time trials are described, which are 3 different manoeuvres for low velocities, executed by both LMI and Robust controllers. In these trials ‘Blue Lady’ velocities, silhouette trajectory and wind data are recorded. Finally the quality of work for both controllers is collected in two tables.

**Keywords:** multivariable system control; linear matrix inequalities; robust control;  $H_\infty$  matrix norm and  $H_2$  matrix norm

## 1. Introduction

Steering the motion of a sea-going ship is one of the most difficult control problems. The main reason is related to the strongly non-linear and non-stationary characteristics of such objects (see e.g., [1]). Additionally, external disturbances play an important role in the whole regulation process since they change reaction of the vessel to steering signals.

There are a few ways to classify control systems used in the area of vessel movement. One of them is the classification in view of the ship’s speed. The discussed control systems can be divided into three types:

1. For exploitation speed i.e., ‘Full ahead’ or a similar one used on open sea:
  - stabilization of heading ([2–5]),
  - trajectory keeping ([6]),
  - turning operations ([7]),
  - roll stabilization ([8,9]),
  - anti collision maneuvers (although ARPA (Automatic Radar Plotting Aid)) systems are more of an advisory than steering type) ([10])
2. For low speed i.e., ‘Slow or Very Slow ahead’ and ‘Slow or Very Slow Astern’ used mainly in constrained areas:

- controlled motion with any drift angle (crab-wise motion) e.g., during berthing, passing narrow channels etc. ([11]),
  - controlled movement following ROV (Remotely Operated Vehicle) unit ([12]).
3. For speed close to zero:
- dynamic stabilization of position DSP ([12]),
  - stabilization of ship placement in relation to the hydrodynamic structure, position mooring (e.g., Weather Vaning) ([12]).

From control theory point of view the first class of systems mainly consists of one-dimensional regulators (SISO ones). Although they seem to be rather simple regulators that due to non-linear and non-stationary properties of the ship they often lead to modern and very sophisticated solutions e.g., adaptive or robust controllers.

The second and third class presented above belong to the multi-dimensional types of regulators (the MIMO ones) due to the necessity to steer a few of ship's velocities simultaneously. Presented paper concentrates on the controllers for small velocities (It should be pointed out that class 2 and class 3 are similar in the sense that they both deal with several velocities. But approaching the controller synthesis in both classes is definitely different. The reason is related to different properties of the ship dynamics when the vessel is at rest or when it moves with non-zero velocity.).

Steering of the ship movement at these velocities in constrained areas is a big challenge for navigational systems due to low accuracy of measuring systems, in turn impacting the precision and safety of ship movement control. Additionally, maneuvering capabilities of ships at low velocities are limited. The power of propulsion systems is relatively small compared to ship mass, which means that a longer time is required to start the movement or change its direction. To achieve precise control of longitudinal, lateral and rotational velocities in such difficult conditions the ship has to be equipped with at least several propulsion systems. At the same time ship's movement parameters are measured by electro-navigational systems which have strong cross feedbacks. Due to the above constraints it is natural to use multidimensional control systems. It needs to be stressed that multidimensional controlled object identification process is crucial for controller synthesis. In recent years numerous publications have been created that describe this process in marine applications, even for a 4 degrees of freedom (4DOF) object as shown in [13]. Another interesting approach is shown in [14] where identification based on Gauss process is described to be effective. In [15] Support Vector Machines (SVM) optimized by an Artificial Bee Colony (ABC) algorithm are shown. The authors of [16] present numerical simulations that show Jang's scheme is an effective and very simple method for identification of the characteristics of ship roll motion and produce relatively reasonable solutions. In the 2019 paper [17] an analysis of two methods was performed, a nonlinear Nomoto model and a maneuvering model group (MMG) model of Yupeng ship were established and verified by the turning trial at sea, then an adaptive neuro-fuzzy inference system (ANFIS) controller was trained by learning the actual ship trial data.

Classical multidimensional ship movement control methods include, among others, Robust Controllers using minimization of  $H_\infty$ , described in [18], and controllers using minimization of  $H_2$  shown in [19], where the authors solve ship autopilot synthesis problems analytically by tuning a corrector to achieve precise ship movement control. With the increase of interest in the above optimal control methods, the interest in numerical methods is also rising, among them Linear Matrix Inequalities that can be used in control system analysis and synthesis. LMI's are described in detail by authors, for example in [20] and in [21]. In [22–24] the authors describe LMI use in multidimensional systems with Fuzzy Logic controllers. In [25] the chapter about applications of a closed loop system shows results of computer simulations for a state space controller controlling the flight path of a missile. In [26] the authors use a Robust LMI controller with  $H_\infty$  that includes uncertainties, while [27–29]

describe  $H_2/H_\infty$  norm minimization in controller synthesis. Finally [30] show a comparison of  $\mu$  synthesis and LMI controllers where the controlled object was a ship.

Controller synthesis methods, related to marine industry, presented in majority of publications are purely theoretical or based on computer simulations. The very few publications dealing with actual ships or ship models focus on single dimensional control, trajectory control responsible for moving the ship over a set path. Publications from Rolls Royce [31] and Kongsberg [32] describe much more complex multidimensional control in MASS 4 standard but being published by industrial companies do not contain information about used control methods. In comparison this paper describes multidimensional control of a ship model during actual sea trails with a detailed description of methods used.

One of the main reasons to adopt the two mentioned approaches (Robust and LMI) to steer the ship was the necessity of fulfilling condition of stability of the whole control system. In multidimensional systems it is not (in general) so easy to prove. In case of Robust controller system stability (and also robust performance) is related to the special form of  $H_\infty$  norm value called structured uncertainty  $\mu$  Condition  $\mu < 1$  guarantees stability [33]. In case of LMI approach one can choose the area (in the left-hand complex plane) to place poles of the closed control system to fulfil the stability condition. Other advantages (taken into account by the authors) were stable and effective algorithms contained in Matlab/Simulink package. They allowed fully multidimensional controllers to simultaneously steer all ship's thrusters.

## 2. Controlled Object

As a controlled object to verify described regulators one chose an autonomous floating model of a sea-going vessel. It is used for training navigators in different navigational situations e.g., passing narrow channels, berthing, mooring etc.

The vessel named 'Blue Lady' is used by the Foundation for Safety of Navigation and Environment Protection at the Silm lake near Ilawa in Poland (see Figure 1). It is an isomorphous model of a VLCC tanker, built from epoxy resin laminate in 1:24 scale. It is equipped with batteryfed electric drives and a two persons control steering post at the stern. Model actuators are driven by DC electric motors and powered by a batteries pack. They are: one main engine, one aft rudder (blade rudder), two tunnel thrusters (fore and aft), two rotating pump thrusters (fore and aft).

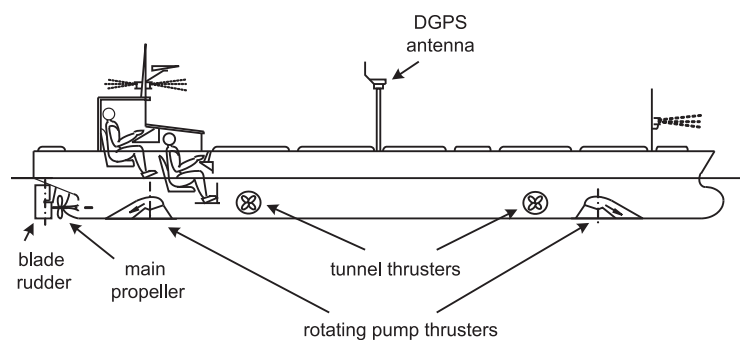


Figure 1. The outline of the training ship 'Blue Lady'.

The silhouette of the ship is presented in Figure 2.



Figure 2. Picture of lardboard the training ship 'Blue Lady'.

The main parameters of the ship are as follows:

Length over all	$L_{OA} = 13.78[m]$
Beam	$B = 2.38[m]$
Draft (average) - load condition	$T_l = 0.86[m]$
Displacement - load condition	$\Delta_l = 22.83[t]$
Speed	$V = 3.10[kn]$

The high-fidelity, fully coupled, nonlinear simulation model of this ship was built for controllers synthesis using the Matlab package. Special attention was paid to proper modeling of the ship's behavior during movement with any drift angle (e.g., astern or askew). The full description of the model can be found in [3,34–36].

Ship motion parameters and environmental disturbances are measured by navigational equipment installed on board:

- Anschütz Standard 20 gyrocompass,
- GILL WindObserver II ultrasonic anemometer,
- LEICA DGPS System 500 receiver working in HPN (High Precision Network) mode.

This equipment communicates with the measurement system using serial communication links in NMEA-0183 standard.

During ship dynamics modeling, for controller synthesis, linearization of the model around it's working point was used. The model identification process took into consideration:

- propulsion operation,
- ship hull construction,
- stationary Kalman filter system (this system is used for  $u, v, r$  velocities recreation) ('Blue Lady' ship model was not equipped with equipment for measuring linear velocities thus the need for Kalman filter system),
- power distribution system used for calculating three components of vector:

$$u = [\tau_x, \tau_y, \tau_r]^T \quad (1)$$

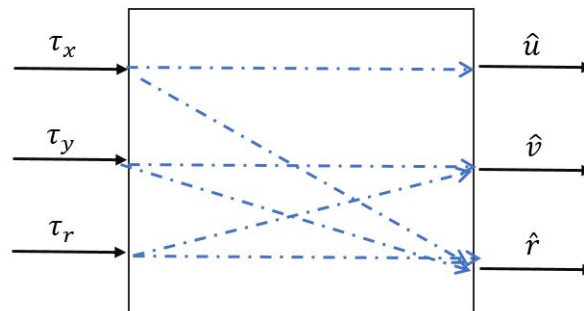
to vector T with seven components of propulsion systems control signals ( $ng_c, \sigma_c, sstd_c, sstr_c, ssod_c, \alpha_{dc}, ssorc, \alpha_{rc}$ ). The details, symbols and ranges of these signals are presented in Table 1. Allocation is not directly the topic of this paper and as such is described in detail in [37]

**Table 1.** Characteristics of the input signals for ship's propellers and rudder [11].

No	Signal	Symbol	Range	Unit
1	revolutions of the main propeller	$ng_c$	[−200–480]	[rpm]
2	conventional rudder angle	$\delta_c$	[−35–35]	[deg]
3	relative thrust of the bow tunnel thr.	$sstd_c$	[−1–1]	[−]
4	relative thrust of the stern tunnel thr.	$sstr_c$	[−1–1]	[−]
5	relative thrust of the bow pump thr.	$ssod_c$	[0–1]	[−]
6	turn angle of the bow pump thr.	$\alpha_{dc}$	[−120–120]	[deg]
7	relative thrust of the stern pump thr.	$ssor_c$	[0–1]	[−]
8	turn angle of the stern pump thr	$\alpha_{rc}$	[60–300]	[deg]

Symbols shown in the third column are used throughout the whole paper.

Controlled object has three input signals:  $\tau_x$ ,  $\tau_y$ ,  $\tau_r$  and three output signals  $\hat{u}$ ,  $\hat{v}$ ,  $\hat{r}$ , relation between these signals is shown on Figure 3 Where:  $[\tau_x]$ —required force (thrust) on the ships longitudinal axis,  $[\tau_y]$ —required force (thrust) on the ships lateral axis,  $[\tau_r]$ —required rotational force,  $[\hat{u}]$ —derivative longitudinal velocity,  $[\hat{v}]$ —derivative lateral velocity and  $[\hat{r}]$ —derivative rotational velocity].

**Figure 3.** Corelation with signals.

During the identification process numerical values of ‘Blue Lady’ model coefficients were calculated, that have been shown in Table 2.

**Table 2.** Ship model coefficients values.

Coeff.	Value Min.	Value Max.	Mean Value
$a_{uu}$	$-5.99 \times 10^{-3}$	$-0.72 \times 10^{-3}$	$-3.36 \times 10^{-3}$
$a_{vv}$	$-1.40 \times 10^{-2}$	$-0.40 \times 10^{-2}$	$-9.00 \times 10^{-3}$
$a_{vr}$	$-2.00 \times 10^{-4}$	-	$-2.00 \times 10^{-4}$
$a_{ru}$	$-3.00 \times 10^{-3}$	-	$-3.00 \times 10^{-3}$
$a_{rv}$	$-1.00 \times 10^{-2}$	-	$-1.00 \times 10^{-2}$
$a_{rr}$	$-1.18 \times 10^{-2}$	$-0.37 \times 10^{-2}$	$-7.75 \times 10^{-3}$
$b_{uu}$	$2.11 \times 10^{-3}$	$6.12 \times 10^{-3}$	$3.62 \times 10^{-3}$
$b_{uv}$	$2.06 \times 10^{-3}$	-	$2.06 \times 10^{-3}$
$b_{vr}$	$-1.28 \times 10^{-5}$	$4.49 \times 10^{-5}$	$1.61 \times 10^{-5}$
$b_{ru}$	$3.00 \times 10^{-5}$	-	$3.00 \times 10^{-5}$
$b_{rv}$	$1.15 \times 10^{-5}$	-	$1.15 \times 10^{-3}$
$b_{rr}$	$8.00 \times 10^{-5}$	-	$8.00 \times 10^{-3}$

After including mean values of these coefficients the calculated state space model became a nominal (mean) model whose state space and output equations are shown below:

$$\begin{bmatrix} \dot{x}_1 \\ \dot{x}_2 \\ \dot{x}_3 \end{bmatrix} = \begin{bmatrix} a_{uu} & 0 & 0 \\ 0 & a_{vv} & a_{vr} \\ a_{ru} & a_{rv} & a_{rr} \end{bmatrix} \times \begin{bmatrix} x_1 \\ x_2 \\ x_3 \end{bmatrix} + \begin{bmatrix} b_{uu} & 0 & 0 \\ 0 & b_{vv} & b_{vr} \\ b_{ru} & b_{rv} & b_{rr} \end{bmatrix} \times \begin{bmatrix} \tau_x \\ \tau_y \\ \tau_r \end{bmatrix}$$

$$\begin{bmatrix} u \\ v \\ r \end{bmatrix} = \begin{bmatrix} 1 & 0 & 0 \\ 0 & 1 & 0 \\ 0 & 0 & 1 \end{bmatrix} \times \begin{bmatrix} x_1 \\ x_2 \\ x_3 \end{bmatrix} \quad (2)$$

Matrices **A**, **B** and **C** of the controlled object, 'Blue Lady' training ship, have the below form:

$$\mathbf{A} = \begin{bmatrix} -3.36 \times 10^{-5} & 0 & 0 \\ 0 & -9.0 \times 10^{-3} & -2.0 \times 10^{-4} \\ -3.0 \times 10^{-3} & -1.0 \times 10^{-2} & -7.75 \times 10^{-3} \end{bmatrix} \quad (3)$$

$$\mathbf{B} = \begin{bmatrix} 3.62 \times 10^{-3} & 0 & 0 \\ 0 & 2.06 \times 10^{-3} & -1.28 \times 10^{-5} \\ 3.0 \times 10^{-5} & 1.15 \times 10^{-5} & 8.0 \times 10^{-3} \end{bmatrix} \quad (4)$$

$$\mathbf{C} = \begin{bmatrix} 1 & 0 & 0 \\ 0 & 1 & 0 \\ 0 & 0 & 1 \end{bmatrix}; \mathbf{D} = \begin{bmatrix} 0 & 0 & 0 \\ 0 & 0 & 0 \\ 0 & 0 & 0 \end{bmatrix} \quad (5)$$

The ship is equipped with several thrusters and a blade rudder (see Figure 1). Hence the 8 input signals can be used in a control system synthesis. The details of these signals are presented in Table 2.

Presented model of ship dynamics was supplemented by the models of dynamics of thrusters and blade rudder, Kalman filters for reconstruction of ship velocities and models of forces driving from wind.

### 3. Robust Controller

#### 3.1. The Augmented Plant

One of the latest approaches is based on minimization of matrix norm  $H_\infty$  (see e.g., [33]) and is shortly described below.

The feedback controller design can be formulated using the concept of uncertainties and weighting functions. It is a convenient way of introducing unmodelled object dynamics and different signal specifications into a MIMO process:

- such quantities can be used for different purposes e.g., establishing the requirements for control quality, description of disturbances, introduction of the influence of non-modelling dynamics of the plant etc.,
- the signals scaling operation is easy to perform by means of weighting functions,
- one can distinguish between more and less important components of the signals vectors (e.g., in errors vector) by proper gain coefficients,
- designer requirements related to the particular signals can be formulated for specified frequency ranges in a natural way.

In the classic control theory the assumed steering quality is only achieved when the plant model is accurate. If the real plant differs (e.g., due to operating conditions) from the model used during controller synthesis this quality can be significantly poorer. The differences between the object and the model are usually named system uncertainties. There are several sources of uncertainties:



Matrix  $\mathbf{P}$  is called the augmented plant (model plant) due to all weighting functions included in it. Introducing the input vector  $\mathbf{d} = [\tilde{\mathbf{r}} \ \tilde{\mathbf{p}} \ \tilde{\mathbf{n}}]^T$  and the weighting error vector  $\mathbf{e} = [\mathbf{e}_y \ \mathbf{e}_u]^T$  one can write:

$$\begin{bmatrix} \mathbf{e} \\ \mathbf{v} \end{bmatrix} = \mathbf{P} \times \begin{bmatrix} \mathbf{d} \\ \mathbf{u} \end{bmatrix} \quad (12)$$

$$\mathbf{u} = \mathbf{K} \times \mathbf{v} \quad (13)$$

The last two equations with the matrix of the pure uncertainties  $\Delta$  enable to build the generalized configuration of the control system shown in Figure 5.

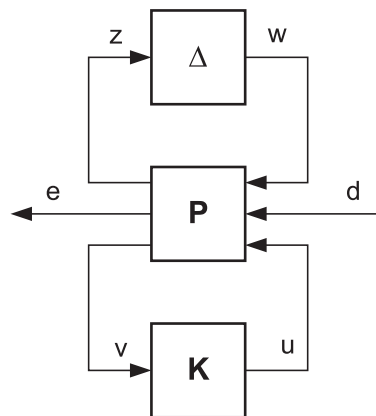


**Figure 5.** The generalized closed-loop system configuration with uncertainties.

### 3.2. The Controller Synthesis

The augmented plant  $\mathbf{P}$  consists of the nominal object model  $\mathbf{G}_n$  and of all matrices of weighting functions (modeling the performance requirements, forming input signals and describing the uncertainties).

The weighting error vector can be expressed in the form:

$$\mathbf{e} = \mathbf{T}_{ed}(\mathbf{P}, \mathbf{K}) \cdot \mathbf{d} \quad (14)$$

where matrix  $\mathbf{T}_{ed}$  can be obtained by means of the Lower Linear Fractional Transformation (see [38]).

The control system synthesis can be treated as a process of calculating a controller  $\mathbf{K}$  which maintains small certain weighted signals (e.g., control errors) under assumption that the changes of the plant (ship) properties are inside the determined area (described by weighting functions of uncertainties). One of the possible ways to define the ‘smallness’ of signals (or transfer matrices) are matrix norms  $H_\infty$  (see e.g., [39]) expressed by the following equations:

$$\|\mathbf{T}_{ed}(\mathbf{s})\|_\infty = \max_{\omega \in (0, \infty)} \bar{\sigma}[\mathbf{T}_{ed}(j\omega)] \quad (15)$$

The algorithm named ‘D-K iteration’ from Matlab was used to compute the robust  $H_\infty$  controller for the system presented in Figure 4. The obtained controller in state model form was of high order equal to 41—the same as the open-loop system. The stability of the whole closed-loop control system is ensured by execution of the modified Small Gain Theorem. For described system (given by matrix  $\mathbf{T}_{ed}$ ) with uncertainties one can couch so called Structured Singular Value— $\mu_{\mathbf{T}_{ed}}$  (see Equation (15)). Without a loss in generality, when  $\mu_{\mathbf{T}_{ed}}$  is smaller the 1, the control system is internally stable (more details one can found in Skogestad and Postlethwaite (2003) with the proofs of the proper theorems).

The value of  $H_\infty$  norm was  $0.56 < 1$  which ensures the robust property of the controller.

The order reduction procedures were performed to decrease this order (without the decline of robust property). Finally a controller of the 21st order was obtained.

The description of the whole procedure named ‘D-K iteration’ and ‘Optimal Hankel Norm Approximation’ essential to obtain the Robust controller is too extensive for presented article, therefore only the set of conditions was presented. The procedures were described in details in the paper: [40].

#### 4. LMI Controller

##### 4.1. The LMI Concept and the Formulation of the Plant

Linear Matrix Inequalities are a convex optimization tool used, among others, for controller synthesis based on robust control ([20]). Based on LMI’s canonical form:

$$\mathbf{F}(x) = \mathbf{F}_0 + \sum_{i=1}^m \mathbf{F}_i \cdot x_i \succ 0 \quad (16)$$

where:

- decision variable vector (unknown)  $x = [x_1, x_2, \dots, x_m]^T \in R^m$ ,
- matrices marked as  $\mathbf{F}_0 \dots \mathbf{F}_i \in R^{n \times n}$  are real and symmetrical,
- the term “ $\succ 0$ ” means that the matrix  $\mathbf{F}(x)$  is positively defined.

Lyapunov noticed that the necessary and sufficient condition for a linear system to be asymptotically stable is finding a symmetrical positively defined matrix  $\mathbf{P} = \mathbf{P}^T$ ,  $\mathbf{P} \succ 0$  (The problem of finding a symmetrical, positively defined matrix  $\mathbf{P}$  is often called the feasibility problem.) ( $\mathbf{P}$  is the unknown variable) while fulfilling the Lyapunov inequality:

$$\mathbf{A}^T \mathbf{P} + \mathbf{P} \mathbf{A} \prec 0 \quad (17)$$

Combining the above condition about the feasibility problem with  $\mathbf{P} \succ 0$  relation the LMI stability condition can be formed:

$$\begin{bmatrix} -\mathbf{A}^T \mathbf{P} - \mathbf{P} \mathbf{A} & 0 \\ 0 & \mathbf{P} \end{bmatrix} \succ 0 \quad (18)$$

where matrix  $\mathbf{A}$  is the controlled object and matrix  $\mathbf{P}$  is the unknown.

This problem is described in [20,21,25,41]. The ‘Blue Lady’ multidimensional model is described in detail also in e.g., [42]. The controller synthesis method for a state space controller for above ship model is shown in [36,43]. Based on simulation results controller structure based on a state space controller was chosen, as:

$$u = \mathbf{K} \cdot x_{zk}, \quad (19)$$

Closed loop system state space equations have the form of (due to the complexity of the problem, in this part the sizes of specific matrices have not been given. However state space variable  $x_{zk}$  is composed of state space variables of the inertial element and controlled object):

$$\begin{cases} \dot{x}_{zk} = (\mathbf{A}_{cl} + \mathbf{B}_u \mathbf{K})x_{zk} + \mathbf{B}_w w, & x_{zk} = \begin{bmatrix} x_i \\ x \end{bmatrix}, \\ z = (\mathbf{C}_z + \mathbf{D}_{zu} \mathbf{K})x_{zk} + \mathbf{D}_{zw} w \\ z_\infty = (\mathbf{C}_\infty + \mathbf{D}_{\infty u} \mathbf{K})x_{zk} + \mathbf{D}_{\infty z} w \\ z_2 = (\mathbf{C}_2 + \mathbf{D}_{2u} \mathbf{K})x_{zk} + \mathbf{D}_{2w} w, \end{cases} \quad (20)$$

where:

- $\mathbf{A}_{cl}$ —controlled object state space matrix, represents system dynamics;
- $\mathbf{B}_u$ —control matrix of control ‘ $u$ ’ signal ;

- $B_w w$ —control matrix of input ‘ $w$ ’ signal ;
- $C_z$ —output matrix of output signal ‘ $z$ ’;
- $C_\infty$ —output matrix of ‘ $z_\infty$ ’ signal;
- $C_2$ —output matrix of ‘ $z_2$ ’ signal;
- $D_{zu}$ —transition matrix of ‘ $z$ ’ and ‘ $u$ ’ signals;
- $D_{zw}$ —transition matrix of ‘ $z$ ’ and ‘ $w$ ’ signals;
- $D_{\infty u}$ —transition matrix of ‘ $z_\infty$ ’ and ‘ $u$ ’ signals;
- $D_{\infty w}$ —transition matrix of ‘ $z_\infty$ ’ and ‘ $w$ ’ signals;
- $D_{2u}$ —transition matrix of ‘ $z_2$ ’ and ‘ $u$ ’ signals;
- $D_{2w}$ —transition matrix of ‘ $z_2$ ’ and ‘ $w$ ’ signals;
- ‘ $z_\infty$ ’ and ‘ $z_2$ ’—additional output signals necessary for calculations of  $H_\infty$  and  $H_2$  norms.

Where matrices  $A_{cl}$ ,  $B_w w$  and  $B_u$  have the form of:

$$A_{cl} = \begin{bmatrix} A_{in} - B_{in}DC_{in} & -B_{in}C \\ B_{np1}C_{in} & A_{np1} \end{bmatrix}, B_w w = \begin{bmatrix} B_{in} \\ 0_{[3 \times 3]} \end{bmatrix}, B_u = \begin{bmatrix} B_{in}D \\ B_{np1} \end{bmatrix}.$$

In the following sections of this paper the authors will often relate to state space equations of the closed loop system (20) in which matrices have been defined taking into account parametric uncertainties  $A_{np1}$ ,  $B_{np1}$  with a first order inertial element included in the system (described with matrices  $A_{in}$ ,  $B_{in}$ ,  $C_{in}$  and  $D_{in}$ ). Figure 6 shows a simplified block diagram of the control system with an LMI state space controller.

Structure of the closed loop system from Figure 6 includes input signal vector  $w$ , control signal vector  $u$  and output signal vectors  $z, z_2, z_\infty$ .

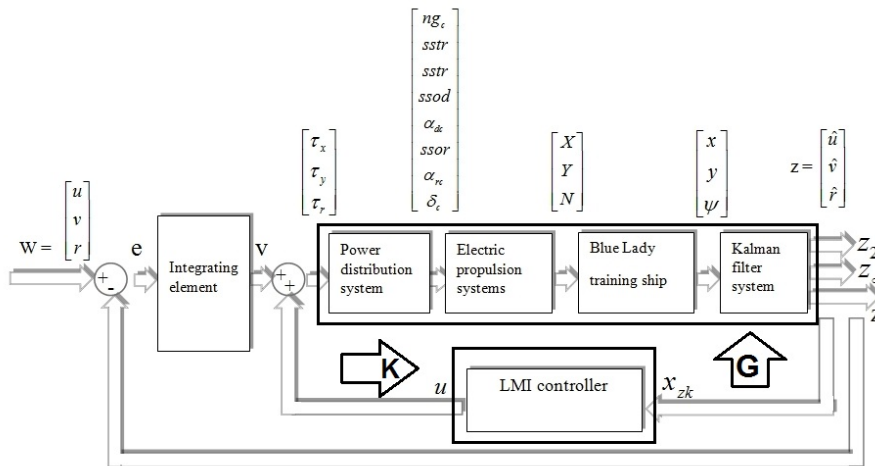


Figure 6. Simplified block diagram of the closed loop control system.

However,  $z_\infty$  and  $z_2$  signal vectors are symbolic and have been implemented in state space equations in order to determine  $H_\infty$  and  $H_2$ . The methodology of the controller synthesis based on Linear Matrix Inequality consists of a few steps which have to be fulfilled simultaneously.

#### 4.2. Stability Restriction—Poles in the Left Half-Plane of Complex Variable Plane $s$

The first stage is to define the pole placement region located in the left half-plane of complex variable plane  $s$  in order to specify dynamic parameters of the designed closed loop system. First LMI condition:

$$R_D(A, X_D) = L \otimes X_D + M \otimes (AX_D) +$$

$$+ \mathbf{M}^T \otimes (\mathbf{A}\mathbf{X}_D)^T \prec 0 \quad (21)$$

is fulfilled if and only if there exists a symmetrical positively defined matrix  $\mathbf{X}_D$ . where:

- $\mathbf{A}$ —in this specific case instead of matrix  $\mathbf{A}$  we have to use the form  $= (\mathbf{A}_{cl} + \mathbf{B}_u\mathbf{K})$ , has to be used,
- $\mathbf{X}_D$ —the unknown, symmetrical positively defined Lyapunov matrix  $\mathbf{X} \succ 0, \mathbf{X} = \mathbf{X}^T$ ,
- $\mathbf{L}, \mathbf{M}$ —specific, user defined matrices.

The choice of the shape of the convex region and its parameters (e.g., circle with diameter  $r$  and center  $q$  or location of vertical stripes  $a_1$  and  $a_2$ ) was done empirically by the user. Influence of pole placement on controller parameters is shown in [25,44,45].

#### 4.3. Minimization of $H_\infty$ Matrix Norm

The second stage is  $H_\infty$  minimization related to an estimation of scalar value  $\gamma_\infty$  which is the upper limit of the  $H_\infty$  norm. When determining the smallest value of  $\gamma_\infty$  for the given pole placement region of the closed loop system, it was assumed that the obtained scalar value  $\gamma_\infty$  is constant. Scalar value  $\gamma_\infty$  can be calculated based on  $H_\infty$  minimization or it can be assumed to be a constant limit. Second LMI condition has the form:

$$\begin{bmatrix} \mathbf{A}\mathbf{X}_\infty + \mathbf{X}_\infty\mathbf{A}^T & \mathbf{B} & \mathbf{X}\mathbf{C}^T \\ \mathbf{B}^T & -\gamma_\infty^2\mathbf{I} & \mathbf{D}^T \\ \mathbf{C}\mathbf{X} & \mathbf{D} & -\mathbf{I} \end{bmatrix} \prec 0 \quad (22)$$

The above equation is generic and in this specific case, taking into account Equation (20), it has the below form:

- $\mathbf{A} = (\mathbf{A}_{cl} + \mathbf{B}_u\mathbf{K});$
- $\mathbf{B} = \mathbf{B}_w;$
- $\mathbf{C} = \mathbf{C}_\infty + \mathbf{D}_{u\infty}\mathbf{K}_\infty;$
- $\mathbf{D} = \mathbf{D}_{\infty w}.$

#### 4.4. Minimization of $H_2$ Matrix Norm

The third stage is  $H_2$  norm minimization. One of the ways of obtaining this is to look for  $\gamma_2$ . Assuming that:

$$\gamma_\infty > \gamma_{\infty min} \quad (23)$$

Value  $\gamma_2$  can be obtained using the Pareto Curve (see [29,46,47]). We receive a relation between the set value of  $H_\infty$  norm (and more precisely the minimal value of  $\gamma_\infty$ ) and a minimized value of  $H_2$  norm (which is the value of  $\gamma_2$ ). The third LMI condition:

$$\left\{ \begin{array}{l} \begin{bmatrix} \mathbf{A}\mathbf{X}_2 + \mathbf{X}_2\mathbf{A}^T & \mathbf{B} \\ \mathbf{B}^T & -\mathbf{I} \end{bmatrix} \prec 0 \\ \begin{bmatrix} \mathbf{Q} & \mathbf{C}^T \\ \mathbf{C} & \mathbf{X}_2 \end{bmatrix} \succ 0 \\ \text{Tr}(\mathbf{Q}) < \gamma_2^2, \end{array} \right. \quad (24)$$

is fulfilled if and only if there exists a symmetrical positively defined matrix  $\mathbf{X}_2$  and a symmetrical matrix  $\mathbf{Q}$ . The above equation is generic and in this specific case, taking into account Equation (20), it has the below form:

- $\mathbf{A} = (\mathbf{A}_{cl} + \mathbf{B}_u\mathbf{K});$
- $\mathbf{B} = \mathbf{B}_w;$
- $\mathbf{C} = \mathbf{C}_2 + \mathbf{D}_{2u}\mathbf{K}_2;$
- $\mathbf{D} = \mathbf{D}_{2u}.$

#### 4.5. Last Assumption and Final Controller

The fourth stage uses Theorem 10.1 (25) from [25] where the authors assume that matrix  $\mathbf{X}$  is equal to  $\mathbf{X} = \mathbf{X}_D = \mathbf{X}_2 = \mathbf{X}_\infty$ . In Duan and Yu (2013) there is a following proposition: The problem of finding a controller is possible if and only if the below set:

$$\mathbb{P} = \left\{ (\mathbf{X}_D, \mathbf{Y}_D, \mathbf{X}_2, \mathbf{Y}_2, \mathbf{X}_\infty, \mathbf{Y}_\infty) \in \left\{ \begin{array}{l} (\mathbf{X}_D, \mathbf{Y}_D) \in \Omega_D \\ (\mathbf{X}_2, \mathbf{Y}_2) \in \Omega_2 \\ (\mathbf{X}_\infty, \mathbf{Y}_\infty) \in \Omega_\infty \end{array} \right\}; \dots \right. \\ \left. \dots \mathbf{Y}_D \mathbf{X}_D^{-1} = \mathbf{Y}_2 \mathbf{X}_2^{-1} = \mathbf{Y}_\infty \mathbf{X}_\infty^{-1} \right\} \quad (25)$$

is not null, and in this case, a gain matrix is determined by:

$$\mathbf{K} = \mathbf{Y}_\infty \mathbf{X}_\infty^{-1} = \mathbf{Y}_2 \mathbf{X}_2^{-1} = \mathbf{Y}_D \mathbf{X}_D^{-1}. \quad (26)$$

For parameter set  $\mathbb{P}$  finding the matrix:

$$(\mathbf{X}_D, \mathbf{Y}_D, \mathbf{X}_2, \mathbf{Y}_2, \mathbf{X}_\infty, \mathbf{Y}_\infty) \in \mathbb{P}, \quad (27)$$

is not an LMI problem and therefore might be very difficult to perform. Thus the matrix is defined assuming that:

$$\mathbf{X}_D = \mathbf{X}_2 = \mathbf{X}_\infty \triangleq \mathbf{X}, \quad (28)$$

and

$$\mathbf{Y}_D = \mathbf{Y}_2 = \mathbf{Y}_\infty \triangleq \mathbf{Y}, \quad (29)$$

than parameter set  $\mathbb{P}$  is reduced to:

$$\begin{aligned} \mathbb{P}_0 &= \{(\mathbf{X}, \mathbf{Y}, \mathbf{X}, \mathbf{Y}, \mathbf{X}, \mathbf{Y}); (\mathbf{X}, \mathbf{Y}) \in \Omega_D, (\mathbf{X}, \mathbf{Y}) \in \Omega_2, (\mathbf{X}, \mathbf{Y}) \in \Omega_\infty\} \\ &= \{(\mathbf{X}, \mathbf{Y}, \mathbf{X}, \mathbf{Y}, \mathbf{X}, \mathbf{Y}); (\mathbf{X}, \mathbf{Y}) \in \Omega_D \cap \Omega_2 \cap \Omega_\infty\} \\ &= \{(\mathbf{X}, \mathbf{Y}, \mathbf{X}, \mathbf{Y}, \mathbf{X}, \mathbf{Y}); (\mathbf{X}, \mathbf{Y}) \in \Omega_0\}. \end{aligned} \quad (30)$$

Based on the above relation matrices  $(\mathbf{X}, \mathbf{Y}) \in \Omega_0$  can be found rather than  $(\mathbf{X}_D, \mathbf{Y}_D, \mathbf{X}_2, \mathbf{Y}_2, \mathbf{X}_\infty, \mathbf{Y}_\infty) \in \mathbb{P}$  and gain matrix has the form of:

$$\mathbf{K} = \mathbf{Y} \mathbf{X}^{-1}. \quad (31)$$

This means that LMI conditions formulated for  $H_\infty$  by Equation (22), for  $H_2$  by Equation (24) and for chosen pole placement (Equation (21)) are fulfilled if there exists a symmetrical positively determined Lyapunov Matrix. This assumption (extortion), that all Lyapunov matrices are equal in all variants and that all three LMI conditions are treated as one limitation, allows to perform state space controller synthesis. This "method" leads to the so called "conservative" optimization, which means that some of the conditions will be fulfilled with a large margin (often called a conservative solution). Because matrix  $\mathbf{X}$  is positively determined there exists its converse matrix  $\mathbf{Y}$  and so state space controller matrix  $\mathbf{K}$  can be described as:

$$\mathbf{K} = \mathbf{Y} \mathbf{X}^{-1}. \quad (32)$$

Taking into account proposition (25) a single general LMI condition was formulated (the described area of limitation is marked  $\Omega_0$  on Figure 7) thanks to which the above method allowed to calculate state space controller gain matrix  $\mathbf{K} = \mathbf{Y} \mathbf{X}^{-1}$ .

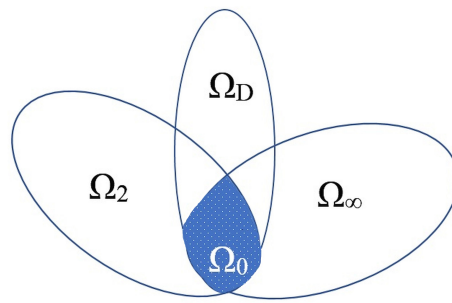


Figure 7. Parameter set  $\Omega_2, \Omega_\infty, \Omega_D$ , areas marker is  $\Omega_0$ .

The final form of state space controller gain matrix  $\mathbf{K}$ , which stabilizes the whole control system and minimizes  $H_\infty$  and  $H_2$  norms, is shown below:

$$\mathbf{K} = \begin{bmatrix} 1498.85 & 0.05 & 0.27 & -799.67 & -0.02 & -0.16 \\ -0.03 & 1696.22 & -5.115 & 0.02 & -952.02 & 3.26 \\ -5.68 & -1.63 & 440.99 & 3.44 & 1.03 & -247.15 \end{bmatrix} \quad (33)$$

The received matrix is a suboptimal solution also know as the conservative solution. It comes from the assumption that  $\mathbf{X} = \mathbf{X}_D = \mathbf{X}_2 = \mathbf{X}_\infty$  and is the sufficient solution.

## 5. Experiments

### 5.1. The Steering Quality Validation

Presented regulators are compared during real - time experiments performed on the lake Silm near Ilawa Poland. The training ship 'Blue Lady' was used as a control object.

A few exemplary results are presented below. The quality of the steering was calculated using two values: mean error of the three velocities (see Equation (34)) and the maximum range of the deviation calculated for the controlled signal in the steady state period of the simulation runs (see Equation (35)):

$$\Delta x[\%] = \frac{\sqrt{\sum_n^1 (x_{given} - x_{control})^2}}{n} \cdot 100, \quad (34)$$

where:  $n$ —number of measurements;  $x$ —deviation value, in percentage, of measured parameter  $x \in u, v, r$ ;  $x_{given}$ —reference signal value (given value)  $x_{control}$ —output signal value received from the system.

$$\Delta_{u,v,r}[\%] = (x_{max} - x_{min}) \cdot 100, \quad (35)$$

where:

- $x_{max}$ —maximum output signal value received from the system,
- $x_{min}$ —minimum output signal value received from the system.

In each of the presented results, called manouvers 1, 2 and 3 respectively, the first figure shows 'Blue Lady' ship model silhouete trajectory in  $x$  and  $y$  coordinate system as measured by the GPS.

The second and third figures show results for both controllers and for comparison reasons both have been done in the same time frame.

All  $[u, v, r]$  velocity graphs also include wind reading, (taken from GILL Wind Observer II) shown in Beaufort scale.

### 5.2. Exemplary Results of Three Exercises

- Maneuver no. 1

Ahead movement with a given longitudinal velocity  $u = 0.1$  [m/s], with maneuver of the duration of 700 [s]. Values of lateral and rotational velocities were set to  $v = 0$  [m/s],  $r = 0$  [deg/s]. This type of ship maneuver, at low velocities, is very common when navigating narrow passages like channels, rivers or entering harbors. Trajectory ship are shown on Figure 8. Results of the Robust controller are shown on Figure 9, and for the LMI controller on Figure 10.

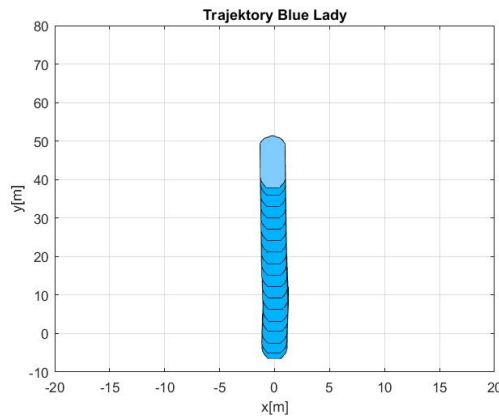


**Figure 8.** Trajectory ship ‘Blue Lady’ for ahead maneuver with longitudinal velocity  $u = 0.1$  [m/s],  $v = 0.0$  [m/s],  $r = 0.0$  [rad/s] and maneuver duration 500 [s].

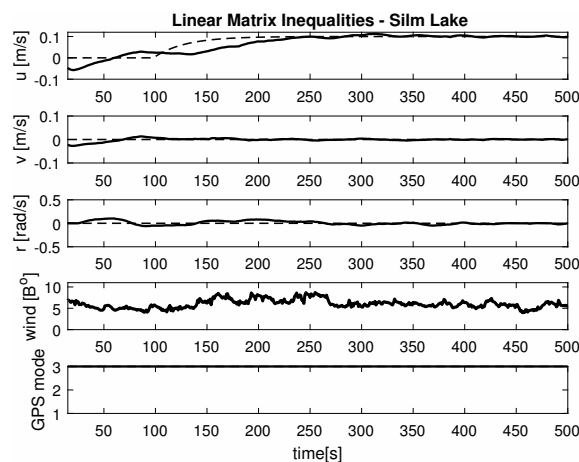


**Figure 9.** Ahead maneuver with longitudinal velocity  $u = 0.1$  [m/s],  $v = 0$  [m/s],  $r = 0$  [rad/s], wind [B°] and GPS mode [-], maneuver duration 500 [s].

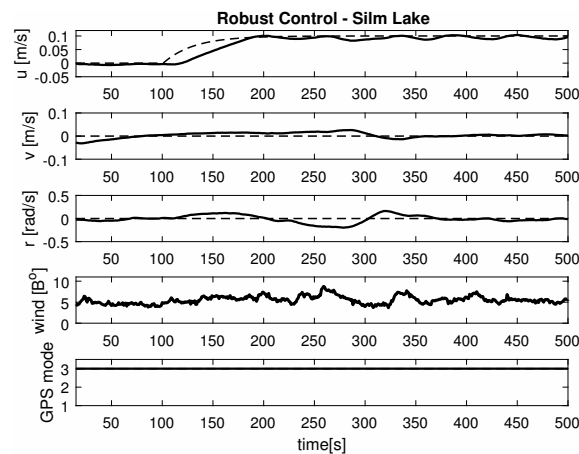


**Figure 10.** Ahead maneuver with longitudinal velocity  $u = 0.1$  [m/s],  $v = 0$  [m/s],  $r = 0$  [rad/s], wind [B°] and GPS mode [-], maneuver duration 500 [s].

- Maneuver no. 2

Ahead and sideways movement with given longitudinal velocity  $u = 0.1$  [m/s] and lateral one  $v = 0.05$  [m/s] with no rotational velocity  $r = 0$  [rad/s] and with maneuver duration of 500 [s]. This type of ship maneuver, at low velocities, is a typical approach to berth which is located parallel to ships. Trajectory ship are shown on Figure 11. Results of the Robust controller are shown on Figure 12 position, and for the LMI controller respectively on Figure 13.

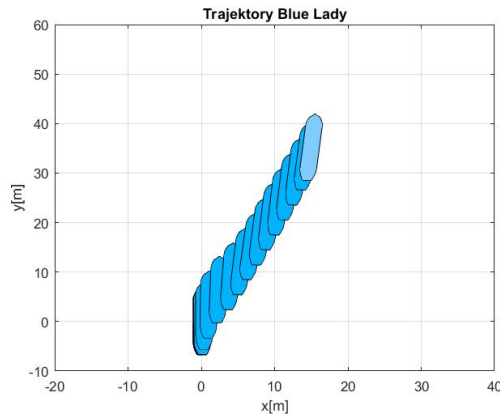


**Figure 11.** Trajectory ship 'Blue Lady' for ahead maneuver with longitudinal velocity  $u = 0.1$  [m/s],  $v = 0.05$  [m/s],  $r = 0.0$  [rad/s], wind [ $B^\circ$ ] and GPS mode [-], maneuver duration 500 [s].

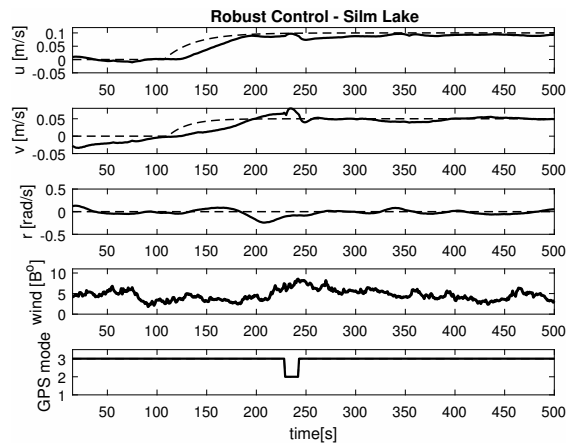


**Figure 12.** Ahead maneuver with longitudinal velocity  $u = 0.1$  [m/s],  $v = 0.05$  [m/s],  $r = 0.0$  [rad/s], wind [ $B^\circ$ ] and GPS mode [-], maneuver duration 500 [s].

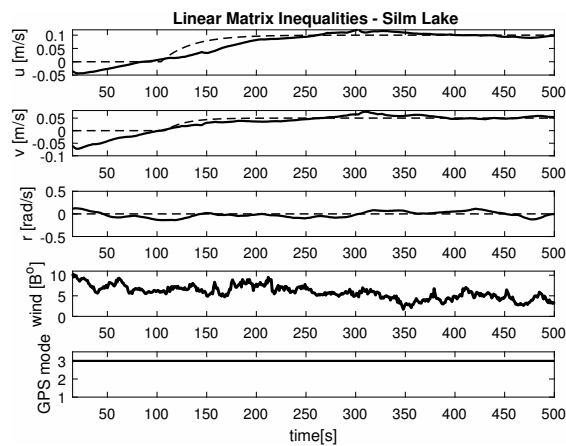


**Figure 13.** Ahead maneuver with longitudinal velocity  $u = 0.1$  [m/s],  $v = 0.05$  [m/s],  $r = 0.0$  [rad/s], wind [ $B^\circ$ ] and GPS mode [-], maneuver duration 1100 [s].

- Maneuver no. 3

Ahead and sideways movement with rotation when performance velocities were set as follows. Duration of the maneuver was 1100 [s]. This type of ship maneuver, at low velocities, is a typical approach to berth which is located perpendicular to ships course. Trajectory ship are shown on Figure 14. Results of the Robust controller are shown on Figure 15, and for the LMI controller on Figure 16.

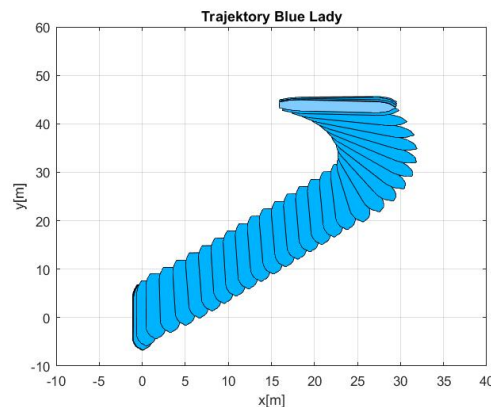


**Figure 14.** Trajectory ship 'Blue Lady' for ahead maneuver with longitudinal velocity  $u = 0.05$  [m/s],  $v = 0.05$  [m/s],  $r = -0.3$  [rad/s] wind [ $B^\circ$ ] and GPS mode [-], maneuver duration 1100 [s].

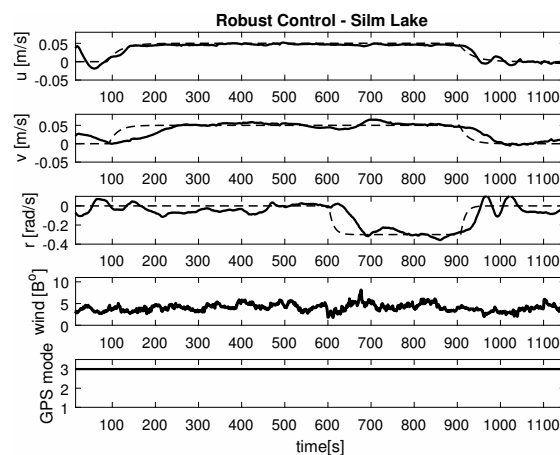


**Figure 15.** Ahead maneuver with longitudinal velocity  $u = 0.1$  [m/s],  $v = 0.05$  [m/s],  $r = -0.3$  [rad/s], wind [ $B^\circ$ ] and GPS mode [-], maneuver duration 1100 [s].

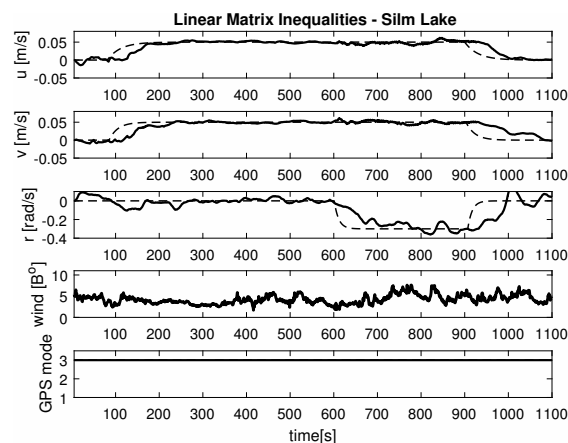


**Figure 16.** Ahead maneuver with longitudinal velocity  $u = 0.05$  [m/s],  $v = 0.05$  [m/s],  $r = -0.3$  [rad/s], wind [ $B^\circ$ ] and GPS mode [-], maneuver duration 1100 [s].

### 5.3. Comparison and Comments

Based on presented Figures 8–16 one can calculate the quality of the work of both controllers. Taking into account formulas (34) and (35) one can create tables (Tables 3 and 4 respectively) where the numerical comparison of Robust controller and LMI one is presented. The main conclusion is as follows: both controllers have similar quality of work but the LMI controller is simpler.

**Table 3.** Comparison of mean deviation from given values describe in (34).

Manoeuvre	Signal	Robust	Linear
		Control Sim Lake	Matrix Inequalities Sim Lake
1	$\Delta_u$ [%]	0.0280	0.0167
2	$\Delta_u$ [%]	0.0385	0.0282
	$\Delta_v$ [%]	0.0249	0.0306
3	$\Delta_u$ [%]	0.0086	0.0088
	$\Delta_v$ [%]	0.0137	0.0079
	$\Delta_r$ [%]	0.0627	0.0760

**Table 4.** Comparison of mean deviation values after a time when received values are different from given values describe in (35).

Manoeuvre	Signal	Robust	Linear
		Control Sim Lake	Matrix Inequalities Sim Lake
1	$\Delta_u$ [%]	2.0897	3.6033
2	$\Delta_u$ [%]	2.3078	3.8103
	$\Delta_v$ [%]	4.0525	3.9736
3	$\Delta_u$ [%]	1.0119	2.2886
	$\Delta_v$ [%]	2.7124	2.0503
	$\Delta_r$ [%]	8.6222	8.8481

The controller matrix size for the Robust controller is [21x14] while for LMI controller it has a dimension of only [3x6]. It proves that using LMI approach according to the assumptions of [25] can reduce the controller size. Simulation results show also that LMI controllers are simple and effective control systems.

It was observed that atmospheric factors, like wind, didn't have a meaningful effect on controller operation. Unfortunately GPS operation mode fluctuations had a severe impact on controller operation. In several areas of Silm Lake the GPS operation mode changed itself which resulted in "repositioning" the ship by several meters in calculations. This effect can be observed on maneuver no. 2 for the Robust controller between 50 [s] and 100 [s] as well as in maneuver no. 3 for Robust controller in 700 [s]. Multidimensional controllers can also be used in small ships used in autonomous transport systems in coastal and inshore waters [48–50].

## 6. Conclusions

This paper presents synthesis methods for a multidimensional Robust controller and a multidimensional LMI controller. Many real experiments have been performed on the lake and examples useful for examining both controllers performance have been presented.

It should be pointed out that both controllers ensure stability of the whole control systems, what it not so obvious (and not easy to prove) in case of multidimensional controllers.

The testing will be done while navigating narrow passages and berthing both parallel and perpendicular to ships heading. It is very instructive to compare the quality of the same manoeuvres performed by experienced ship masters and computers.

**Author Contributions:** Conceptualization, M.R. and W.G.; methodology, M.R. and W.G.; software, M.R. and W.G.; validation, M.R.; formal analysis, W.G.; investigation, M.R. and W.G.; resources, M.R.; data curation, M.R. and W.G.; writing—original draft preparation, M.R.; writing—review and editing, M.R.; visualization, M.R. and W.G.; supervision, W.G.; project administration, W.G.; funding acquisition, M.R. All authors have read and agreed to the published version of the manuscript.

**Funding:** This project is financially supported in part under the framework of a program of the Ministry of Science and Higher Education (Poland) as ‘Regional Excellence Initiative’ in the years 2019–2022, project number 006/RID/2019/MGB/4, amount of funding 11 870 000 PLN.

**Conflicts of Interest:** The author declare no conflict of interest.

## References

1. Fossen, T.I. *Guidance and Control of Ocean Vehicles*; Wiley and Sons: Chichester, UK, 1994.
2. Fossen, T.I.; Perez, T. Kalman filtering for positioning and heading control of ships and offshore rigs. *IEEE Control Syst. Mag.* **2009**, *29*, 32–46.
3. Tomera, M. A multivariable low speed controller for a ship autopilot with experimental results. In Proceedings of the 20th International Conference on Methods and Models in Automation and Robotics (MMAR), Międzyzdroje, Poland, 24–27 August 2015; pp. 17–22.
4. Tomera, M. Swarm intelligence applied to identification of nonlinear ship steering model. In *2015 IEEE 2nd International Conference on Cybernetics (CYBCONF)*; IEEE: Piscataway, NJ, USA, 2015; pp. 133–139.
5. Zhang, X.; Yang, G.; Zhang, Q.; Zhang, G.; Zhang, Y. Improved Concise Backstepping Control of Course Keeping for Ships Using Nonlinear Feedback Technique. *J. Navig.* **2017**, *70*, 1401–1414. [[CrossRef](#)]
6. Kula K.S. Model-based controller for ship track-keeping using neural network. In Proceedings of the IEEE 2nd International Conference on Cybernetics (CYBCONF), Gdynia, Poland, 24–26 June 2015; pp. 178–183.
7. Hu, Z.; Peng, X. Integral nested sliding mode control for ship turning. In Proceedings of the 3rd IEEE International Conference on Communication Software and Networks (ICCSN), Xi’an, China, 27–29 May 2011.
8. Perez T. *Ship Motion Control: Course Keeping and Roll Stabilisation Using Rudder and Fins*; Springer: Berlin, Germany, 2015.
9. Perez, T.; Blanke, M. Ship roll damping control. *Ann. Rev. Control* **2012**, *36*, 129–147. [[CrossRef](#)]
10. Lisowski, J.; Mohamed-Seghir, M. Comparison of Computational Intelligence Methods Based on Fuzzy Sets and Game Theory in the Synthesis of Safe Ship Control Based on Information from a Radar ARPA System. *Remote Sens.* **2019**, *11*, 82. [[CrossRef](#)]
11. Gierusz, W.; Vinh, N.C.; Rak, A. Maneuvering control and trajectory tracking of very large crude carrier. *Ocean Eng.* **2007**, *34*, 932–945. [[CrossRef](#)]
12. Fossen, T.I. *Handbook of Marine Craft Hydrodynamics and Motion Control*; John Wiley and Sons: Hoboken, NJ, USA, 2011.
13. Zhang, G.; Zhang, X.; Pang, H. Multi-innovation auto-constructed least squares identification for 4 DOF ship manoeuvring mode modeling with full-scale trial data. *ISA Trans.* **2015**, *58*, 186–195. [[CrossRef](#)]
14. Ramire, W.; Leong, Z.; Nguyen, H.; Jayasinghe, S.G. Non-parametric dynamic system identification of ships using multi-output Gaussian Processes. *Ocean Eng.* **2018**, *166*, 26–36. [[CrossRef](#)]
15. Zhu, M.; Hahn, A.; Wen, Y. Identification-based controller design using cloud model for course-keeping of ships in waves. *Eng. Appl. Artif. Intell.* **2018**, *75*, 22–35. [[CrossRef](#)]
16. Park, J.; Sung, H.; Ahmad, F.; So, S.H.; Syngellakis, S.; Jung, K.H.; Jang, T.S. A Numerical Identification of Excitation Force and Nonlinear Restoring Characteristics of Ship Roll Motion. *J. Mar. Sci. Technol. Taiwan* **2017**, *25*, 475–481.
17. Zhang, Z.; Zhang, X.; Zhang, G. ANFIS-based course-keeping control for ships using nonlinear feedback technique. *J. Mar. Sci. Technol.* **2019**, *24*, 1326–1333. [[CrossRef](#)]
18. Alfi, A.; Shokrzadeh, A.; Asadi, M. Reliability analysis of  $H_\infty$  control for a container ship in way-point tracking. *Appl. Ocean Res.* **2015**, *52*, 309–316. [[CrossRef](#)]

19. Veremey, E.I.; Korovkin, M.V.; Sotnikova, M.V. Ships' Steering in Accurate Regime Using Autopilot with Special Structure of Control Law. *IFAC-PapersOnLine* **2015**, *48*, 7–12. [[CrossRef](#)]
20. Boyd, S.; El-Ghaoui, L.; Feron, E.; Balakrishnan, V. *Linear Matrix Inequalities in System and Control Theory*; Society for Industrial and Applied Mathematics: Philadelphia, PA, USA, 1994.
21. El Ghaoui, L.; Niculescu, S.L. *Advances in Linear Matrix Inequality Methods in Control*; Society for Industrial and Applied Mathematics: Philadelphia, PA, USA, 2000.
22. Lam, H.K.; Leung, F.H.F. *Stability Analysis of Fuzzy-Model-Based Control Systems*; Springer: Berlin, Germany, 2011; Volume 264, pp. 191–215.
23. Ostertag, E. *Mono- and Multivariable Control and Estimation: Linear, Quadratic and LMI Methods*; Springer Science and Business Media: Berlin, Germany, 2011; Volume 2.
24. Patel, H.R.; Shah, V.A. Stable Fault Tolerant Controller Design for Takagi–Sugeno Fuzzy Model-Based Control Systems via Linear Matrix Inequalities: Three Conical Tank Case Study. *Energies* **2019**, *12*, 2221. [[CrossRef](#)]
25. Duan, G.R.; Yu, H.H. *LMIs in Control Systems: Analysis, Design and Applications*; CRC Press: Boca Raton, FL, USA, 2013.
26. Gao, X.; Teo, K.L.; Duan, G.R.; Wang, N. Robust reliable  $H_\infty$  control for uncertain systems with pole constraints. *Int. J. Innov. Comput. Inf. Control* **2012**, *8*, 3071–3079.
27. Zhang, X.K.; Han, X.; Guan, W.; Zhang, G.Q. Improvement of integrator backstepping control for ships with concise robust control and nonlinear decoration. *Ocean Eng.* **2019**, *189*, 106349. [[CrossRef](#)]
28. Zhang, Q.; Sijun, Y.; Yan, L.; Xinmin, W. An enhanced LMI approach for mixed  $H_\infty/H_2$  flight tracking control. *Chin. J. Aeronaut.* **2011**, *24*, 324–328. [[CrossRef](#)]
29. Balandin, D.V.; Kogan, M.M. Pareto optimal generalized  $H_2$ -control and optimal protection from vibration. *IFAC-PapersOnLine* **2017**, *50*, 4442–4447. [[CrossRef](#)]
30. Joeliyanto, E.; Gani, G.; Putri, N.K. Robust control with linear matrix inequality approach for ship steering problem. In Proceedings of the Instrumentation, Control and Automation (ICA), 2016 International Conference, Bandung, Indonesia, 29–31 August 2016; pp. 126–131.
31. Rolls-Royce. The Next Steps of Remote and Autonomous Ships'. Rolls-Royce Holdings plc. 2018. Available online: <https://www.rolls-royce.com//media/Files/R/Rolls-Royce/documents/customers/marine/ship-intel/aawa-whitepaper210616.pdf> (accessed on 30 March 2020).
32. Kongsberg. Autonomous Ship Project, Key Facts about YARA Birkeland. (OpenDocument) 2019. Available online: <https://www.km.kongsberg.com/ks/web/nokbg0240.nsf/AllWeb/4B8113B707A50A4FC125811D00407045> (accessed on 13 January 2020).
33. Doyle, J.C.; Glover, K.; Khargonekar, P.P.; Francis, B.A. State-space Solutions to Standard  $H_2$  and  $H_\infty$  Control Problems. *IEEE Trans. Autom. Control* **1989**, *34*, 831–847. [[CrossRef](#)]
34. Gierusz, W. Simulation model of the shiphandling training boat “Blue Lady”. In *IFAC Proceedings Volumes*; Elsevier: Amsterdam, The Netherlands, 2001 .
35. Pomirski, J.; Rak, A.; Gierusz, W. Control system for trials on material ship model. *Pol. Marit. Res.* **2012**, *19*, 25–30. [[CrossRef](#)]
36. Rybczak, M. Improvement of control precision for ship movement using a multidimensional controller. *Automatika* **2018**, *59*, 63–70. [[CrossRef](#)]
37. Miller, A.; Rybczak, M. Thrust allocation system for Blue Lady training ship taking into account efficient work of main propeller. *Sci. J. Maritime Univ. Szczecin* **2013**, *36*, 123–130.
38. Redheffer, R.M. On a Certain Linear Fractional Transformation. *J. Math. Phys.* **1960**, *39*, 269–286. [[CrossRef](#)]
39. Skogestad, S.; Postlethwaite, I. *Multivariable Feedback Control—Analysis and Design*; John Wiley and Sons: Chichester, UK, 2003.
40. Gierusz, W. The steering of the ship motion: A  $\mu$  synthesis approach. *Arch. Control Sci.* **2006**, *16*, 87–109.
41. Da Ponte Caun, R.; Assunção, E.; Minhoto Teixeira, M.C.; da Ponte Caun, A. LQR-LMI control applied to convex-bounded domains. *Cogit. Eng.* **2018**, *5*, 1–27. [[CrossRef](#)]
42. Miller, A. Identification of a multivariable incremental model of the vessel. In Proceedings of the 21st International Conference on Methods and Models in Automation and Robotics (MMAR), Miedzyzdroje, Poland, 29 August–1 September 2016; pp. 218–224.
43. Miller, A.; Rybczak, M. Methods of controller synthesis using linear matrix inequalities and model predictive control. *Sci. J. Maritime Univ. Szczecin* **2015**, *43*, 22–28.

44. Nodozi, I.; Rahmani, M. LMI-based model predictive control for switched nonlinear systems. *J. Proc. Control Xi'an* **2017**, *59*, 49–58. [[CrossRef](#)]
45. Xue, A.; Zou, H. Pole placement with LMI constraint of fuzzy descriptor system. *J. Franklin Inst.* **2015**, *352*, 2665–2678.
46. Chiu, W.Y. Multiobjective controller design by solving a multiobjective matrix inequality problem. *IET Control Theory Appl.* **2014**, *8*, 1656–1665. [[CrossRef](#)]
47. Molina-Cristóbal, A.; Griffin, I.A.; Fleming, P.J.; Owens, D.H. Linear matrix inequalities and evolutionary optimization in multiobjective control. *Int. J. Syst. Sci.* **2006**, *37*, 513–522. [[CrossRef](#)]
48. Łebkowski, A.; Smierzchalski, R. Hybrid System of Safe Ship Steering at Sea. In Proceedings of the 9th IEEE International Conference on Methods and Models in Automation and Robotics, Międzyzdroje, Poland, 25–28 August 2003; pp. 263–268.
49. Łebkowski, A. Design of an Autonomous Transport System for Coastal Areas, TRANSNAV. *Int. J. Mar. Navig. Saf. Sea Trans.* **2018**, *12*, 117–124.
50. Łebkowski, A. Analysis of the Use of Electric Drive Systems for Crew Transfer Vessels Servicing Offshore Wind Farms. *Energies* **2020**, *13*, 1466. [[CrossRef](#)]



© 2020 by the authors. Licensee MDPI, Basel, Switzerland. This article is an open access article distributed under the terms and conditions of the Creative Commons Attribution (CC BY) license (<http://creativecommons.org/licenses/by/4.0/>).